



Dariusz Bochenek<sup>1</sup>, Przemysław Niemiec<sup>1\*</sup>, Artur Chrobak<sup>2</sup>  
Grzegorz Ziółkowski<sup>2</sup>, Radosław Zachariasz<sup>1</sup>

<sup>1</sup> University of Silesia, Department of Materials Science, ul. Śnieżna 2, 41-200 Sosnowiec, Poland

<sup>2</sup> University of Silesia, Institute of Physics, ul. Uniwersytecka 4, 40-007 Katowice, Poland

Corresponding author: E-mail: niemiec.przemek@gmail.com

Received (Otrzymano) 28.01.2013

## FERROELECTRIC-FERROMAGNETIC COMPOSITES OF BASED ON $\text{Pb}(\text{Fe}_{1/2}\text{Nb}_{1/2})\text{O}_3$

Ferroelectric-ferromagnetic composites based on ferroelectromagnetic  $\text{PbFe}_{1/2}\text{Nb}_{1/2}\text{O}_3$  powder and ferrite powder (zinc-nickel ferrite- $\text{NiZnFe}$  and zinc-manganese ferrite- $\text{MnZnFe}$ ) were obtained in the presented study. The volume fraction of ferroelectromagnetic powder in the composite PFN- $\text{MnZnFe}$  was equal to 90%, while the ferrite powder fraction was 10%. Synthesis of the components of the ferroelectric-ferromagnetic composite was done by the powder calcination method. Final densification was done by the pressureless sintering method. On the obtained ferroelectric-ferromagnetic composites, XRD investigations were performed as well as investigations of the microstructure, EDS, dielectric, magnetic, internal friction and electrical hysteresis loop. The results of these investigations have shown that the combination of ferroelectromagnetic PFN with magnetic ferrite caused an increase in the value of the dielectric permittivity of the composite. Therefore, the addition of the ferrite ( $\text{Ni}_{1-x}\text{Zn}_x\text{Fe}_2\text{O}_4$ ,  $\text{Mn}_{1-x}\text{Zn}_x\text{Fe}_2\text{O}_4$ ) as an additional component improves the magnetic properties of the PFN-ferrite composite. Taking into account the fact that the electric conductivity of zinc-manganese ferrite ( $\text{MnZnFe}$ ) is higher than the zinc-nickel ferrite ( $\text{NiZnFe}$ ), it seems to be a better material for obtaining composites based on ferrite and PFN powders.

**Keywords:** ferroelectromagnetics, multiferroics, ferroelectric-ferromagnetic composites, PFN ceramics, ferrites

### FERROELEKTRYCZNO-FERROMAGNETYCZNE KOMPOZYTY NA BAZIE $\text{Pb}(\text{Fe}_{1/2}\text{Nb}_{1/2})\text{O}_3$

W pracy otrzymano ferroelektryczno-ferromagnetyczne kompozyty na bazie ferroelektromagnetycznego proszku  $\text{PbFe}_{1/2}\text{Nb}_{1/2}\text{O}_3$  oraz proszku ferrytowego (ferrytu niklowo-cynkowego  $\text{NiZnFe}$  oraz ferrytu manganowo-cynkowego  $\text{MnZnFe}$ ). W kompozycie PFN- $\text{MnZnFe}$  ferroelektromagnetyczny proszek PFN stanowił 90%, natomiast proszek ferrytowy stanowił 10%. Syntetyzowanie składników kompozytów przeprowadzono metodą kalcynacji proszków, natomiast zagęszczanie (spiekanie) zsyntetyzowanego kompozytowego proszku metodą spiekania swobodnego. Przeprowadzono badania rentgenowskie, mikrostrukturalne, EDS, dielektryczne, magnetyczne, tarcia wewnętrzne oraz elektrycznej pętli histerezy. Przeprowadzone badania wykazały, że połączenie ferroelektromagnetyka PFN z magnetycznym ferrytem wywołuje zwiększenie wartości przenikalności elektrycznych kompozytu. Dodatkowe czynniki magnetyczne w postaci ferrytu ( $\text{Ni}_{1-x}\text{Zn}_x\text{Fe}_2\text{O}_4$ ,  $\text{Mn}_{1-x}\text{Zn}_x\text{Fe}_2\text{O}_4$ ) zwiększają magnetyczne właściwości kompozytu PFN-ferryt. Ze względu na dużo wyższe przewodnictwo elektryczne ferrytu cynkowo-manganowego  $\text{MnZnFe}$  do projektowania kompozytów na bazie ferroelektrycznego proszku i proszku ferrytowego należy stosować ferryty cynkowo-niklowe ( $\text{NiZnFe}$ ).

**Słowa kluczowe:** ferroelektromagnetyki, multiferroiki, ferroelektryczno-ferromagnetyczne kompozyty, ceramika PFN, ferryty

## INTRODUCTION

Multiferroics are a type of ferroics which have simultaneously at least two spontaneously ordered subsystems among the following states: ferromagnetic, ferroelectric, ferroelastic and ferrotoroidic [1, 2]. The application capabilities of multiferroics depend mainly on the degree of coupling between specific subsystems (magnetic, electric or elastic).

$\text{PbFe}_{1/2}\text{Nb}_{1/2}\text{O}_3$  (PFN) has a perovskite-type structure with a general formula of  $\text{ABO}_3$ , where positions A of the elementary cell are filled with Pb lead ions, while positions B are incidentally filled with Fe iron and Nb niobium ions [3, 4]. According to the classification by

D. Khomski [5], PFN belongs to type-I multiferroics (with weak coupling of the magnetic and electric subsystems) in which ferroelectricity is related to the shift of ferroelectrically active  $d^0$  ions (Nb) from the center of regular octahedrons -  $\text{O}_6$ , while magnetism is related to the presence of  $d^n$  ions (Fe). PFN is applied as a center for MLCC multilayer ceramic capacitors, resonators, filters, sensors and detectors [6-8].  $\text{NiZnFe}$  ( $\text{Ni}_{0.64}\text{Zn}_{0.36}\text{Fe}_2\text{O}_4$ ) belongs to soft ferrites with high resistance  $\rho$  ( $10^5 \Omega\text{m}$ ) [9]. Its working frequency is included within the range of (50÷1000 MHz) and is used in telecommunication filters, distance sensors and

EMI filters, among others. MnZnFe ( $\text{Mn}_{0.8}\text{Zn}_{0.2}\text{Fe}_2\text{O}_4$ ) has high magnetic permeability  $\mu_i$  (3800) and saturation induction  $B_s$  (545 mT). It is used e.g. as telecom filters and proximity sensors.

In the work, ferroelectric-ferromagnetic composites were obtained based on  $\text{PbFe}_{1/2}\text{Nb}_{1/2}\text{O}_3$  and ferromagnetic ferrite (NiZnFe and MnZnFe) in order to strengthen the coupling of the magnetic and electric subsystems in this type of composite.

## EXPERIMENT

For the purpose of obtaining ferroelectric-ferromagnetic composites, multiferroic powder  $\text{PbFe}_{1/2}\text{Nb}_{1/2}\text{O}_3$  (PFN) was used as well as ferrites with strong ferromagnetic properties: NiZnFe ( $\text{Ni}_{0.64}\text{Zn}_{0.36}\text{Fe}_2\text{O}_4$ ) and MnZnFe ( $\text{Mn}_{0.8}\text{Zn}_{0.2}\text{Fe}_2\text{O}_4$ ). The powder proportions in the ferroelectric-ferromagnetic composites equaled: PFN - 90%, ferrite - 10%. PFN was obtained using the columbite method through powder calcination [10]. The ferrite powders were calcinated in the following conditions:  $1000^\circ\text{C}/4$  h. Weighted in appropriate proportions, the composite components underwent milling in a planetary mill type FRITSH Pulverisette 6, wet in ethanol, for 8 h. Synthesizing of the composite powder was carried out in the following conditions:  $T_{\text{synth}} = 900^\circ\text{C}$  and  $t_{\text{synth}} = 2$  h, while densification (sintering) was conducted at  $T_s = 1050^\circ\text{C}/t_s = 2$  h using the pressureless sintering method. Two ferroelectric-ferromagnetic composites were obtained with the following compositions: 0.9PFN-0.1NiZnFe (PFN-NiZnFe) and 0.9PFN-0.1MnZnFe (PFN-MnZnFe). The final steps of the process were grinding, polishing, removing mechanical stresses by heating and putting silver paste electrodes on the composite sample surfaces.

The XRD tests were carried out at room temperature on a diffractometer by Phillips. The microstructure of test sample fractures was examined on a Hitachi S-4700 SEM field emission scanning microscope with a Noran Vantage EDS system. Dielectric properties tests were performed on a QuadTech1920 LCR meter (at measurement field frequencies from 0.02 to 100 kHz). Magnetic properties measurements were performed using a magnetometer SQUID (MPMS XL-7 Quantum Design) in the range of temperatures from  $-271^\circ\text{C}$  to  $27^\circ\text{C}$  (magnetic field to 7 T) and a magnetic Faraday balance in the range of temperatures from  $27^\circ\text{C}$  to  $827^\circ\text{C}$ . The temperature measurements of the  $Q^{-1}(T)$  internal friction and  $Y(T)$  Young modulus were made by an automatic relaxator with acoustic frequencies of the RAK-3 type.

## EXPERIMENTAL RESULTS AND DISCUSSION

Figure 1 shows the XRD pattern of the PFN material powder, NiZnFe ferrite and PFN-NiZnFe composite at room temperature. The XRD diffraction pattern for the

ferrite powder NiZnFe shows a typical single phase cubic spinel. The diffraction peaks of the PFN component were identified as a tetragonal perovskite structure with a  $P4mm$  space group (JCPDS card no. 032-0522) without a pyrochlore phase. For the PFN-NiZnFe composite, the XRD analysis showed the occurrence of a strong maxima from ferroelectromagnetic PFN and the occurrence of peaks from the second component phase, i.e. from the NiZnFe magnetic ferrite. The XRD analysis also confirmed the lack of foreign phases (e.g. pyrochlore). Similar results were obtained for the PFN-MnZnFe composite.

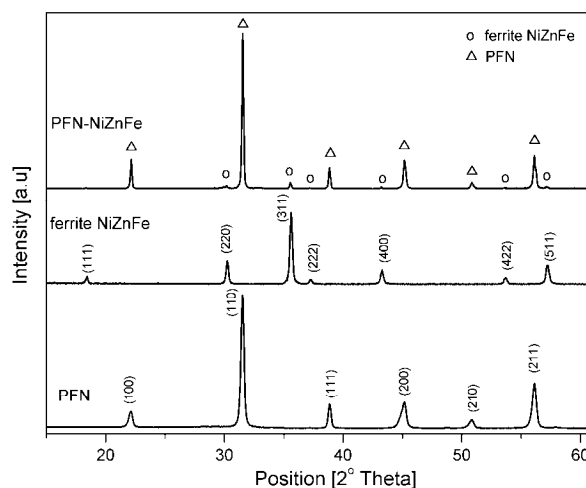


Fig. 1. XRD patterns of PFN-NiZnFe composite, PFN and NiZnFe powders

Rys. 1. Widma rentgenowskie kompozytu PFN-NiZnFe oraz proszków składowych PFN i NiZnFe

Figure 2 shows the EDS tests (Energy Dispersive Spectrometry) of the analyzed composite components (PFN-NiZnFe and PFN-MnZnFe) as well as of specific components (PFN, NiZnFe, MnZnFe). EDS analysis included measurement of ten randomly selected areas of the composite sample fractures. The averaged results of the analysis are summarized in Figure 2. The analysis confirmed the assumed percentage composition of specific components and the occurrence of ferroelectromagnetic (PFN) and ferrite powder elements.

The microstructure of the fracture of the ferroelectric-ferromagnetic composites shows heterogeneity. In the case of the PFN-NiZnFe composite (Fig. 3), the microstructure is composed of grains of the PFN ferroelectric powder with straight boundaries with a polyhedron section. On the other hand, the section of the ferrite powder grains (also with straight boundaries) is (usually) tetrahedral. At the same time, the small grains of the NiZnFe ferrite powder are distributed quite incidentally, they are surrounded by larger PFN grains. The fracture microstructure of the PFN-MnZnFe composite shows considerably larger structure heterogeneity in the whole volume of the sample when compared to PFN-NiZnFe. It contains very large as well as small grains (Fig. 3b).

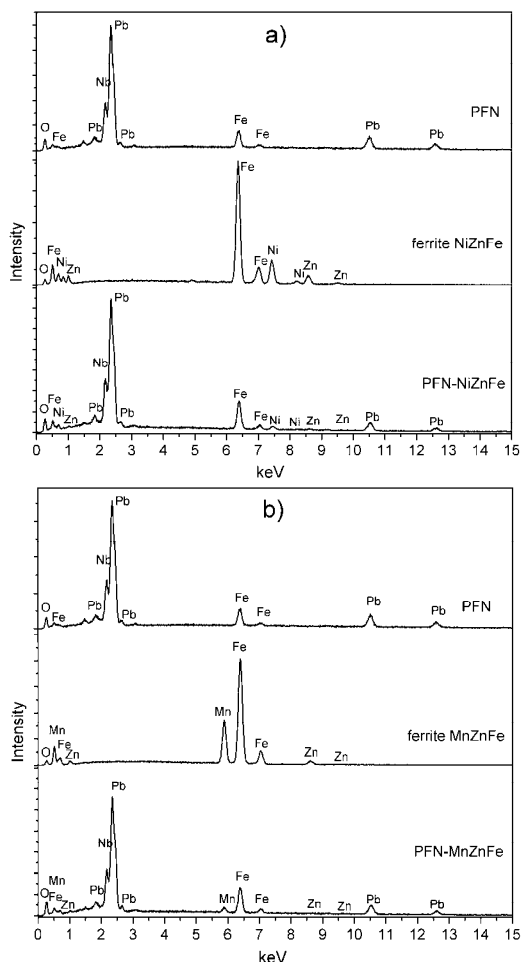


Fig. 2. Images EDS analysis of content element for: a) PFN, NiZnFe, PFN-NiZnFe and b) PFN, MnZnFe, PFN-MnZnFe  
 Rys. 2. Obrazy analizy EDS zawartości pierwiastków dla: a) PFN, NiZnFe, PFN-NiZnFe oraz b) PFN, MnZnFe, PFN-MnZnFe

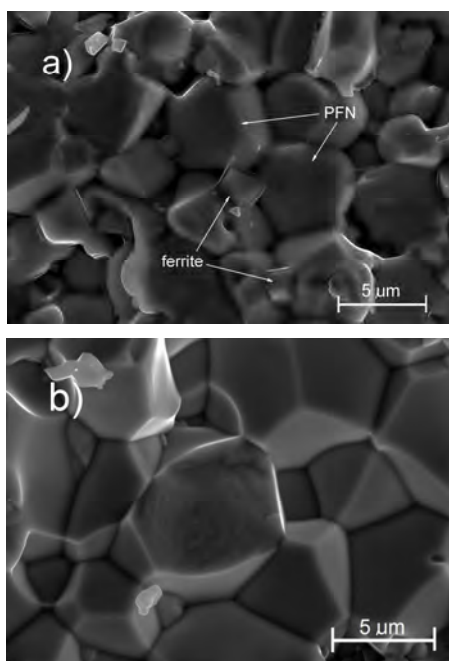


Fig. 3. SEM images of fracture microstructure of composite samples: a) PFN-NiZnFe, b) PFN-MnZnFe  
 Rys. 3. Obrazy SEM mikrostruktury przełamania próbek kompozytu: a) PFN-NiZnFe, b) PFN-MnZnFe

The PFN ceramics have a diffusion phase transition without frequency dispersion. The value of maximum dielectric permittivity  $\epsilon_m$  at temperature Curie  $T_m$  equals approximately 9,000 (dashed line presented in Figure 4a, b - for 1.0 kHz) [10].

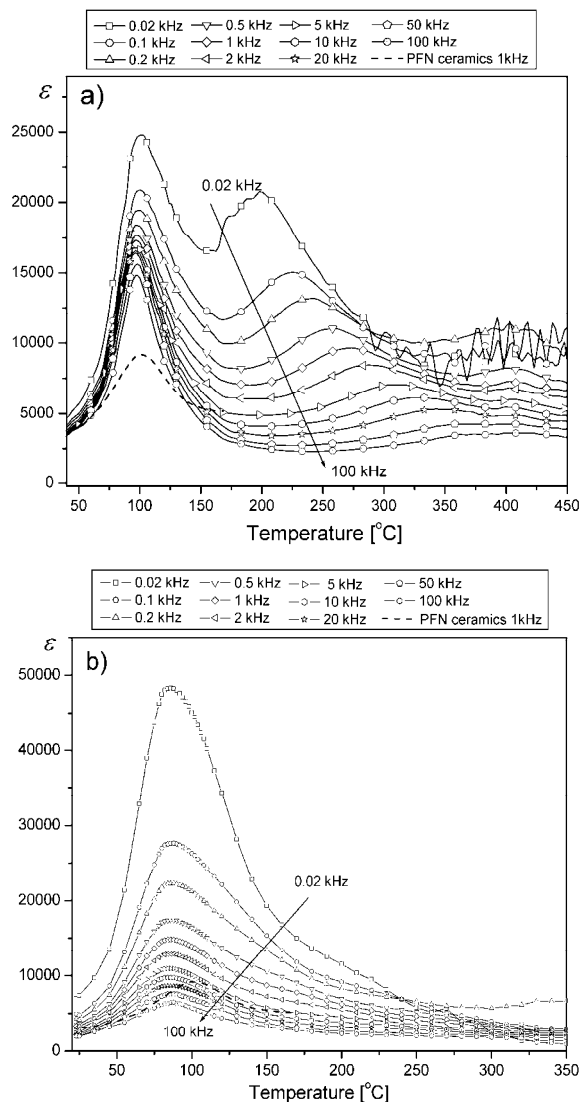


Fig. 4. Temperature dependences of dielectric permittivity  $\epsilon$  for composites: a) PFN-NiZnFe, b) PFN-MnZnFe (heating)  
 Rys. 4. Temperaturowe zależności przenikalności elektrycznej  $\epsilon$  dla kompozytu: a) PFN-NiZnFe, b) PFN-MnZnFe (grzanie)

Compared to the PFN ceramics [10], the PFN-NiZnFe composite with a 10% content of NiZnFe ferrite has higher values of  $\epsilon_m$  at temperature Curie  $T_m$  by approximately 60% (Fig. 4a). At the same time, a decrease in the diffusion of the electric subsystem phase transition is observed. At higher temperatures on diagrams  $\epsilon(T)$ , there is also a second (diffusion) maximum, strongly dependent on the frequency of the measuring field. This phenomenon is perhaps associated with the growth of the electrical conduction (with activation mechanism of electric conductivity). At about 390°C, a third maximum (little anomalies seen in low frequencies) can be observed, associated with the appearance of

the magnetic subsystem phase transition in this area. This phenomenon shows the influence of the magnetic subsystem on the electric properties of the PFN-NiZnFe composite.

In the case of the PFN-MnZnFe composite with a 10% content of ferrite, values  $\varepsilon_m$  at temperature Curie  $T_m$  are even higher, with a larger diffusion of the phase transition. The electric conductivity could be involved in the observed transformation of the dielectric properties temperature dependence. Extremely high values of dielectric permittivity in the PFN-MnZnFe composite are related also to the effect of the magnetic subsystem on the dielectric properties in the area of the phase transition of the electric subsystem. This is a result of the lower temperature of the magnetic phase transition of the MnZnFe ferrite (about 255°C) as compared to NiZnFe (about 400°C), as well as of the narrow range between the phase transition temperatures of the electric and magnetic subsystems. The effect of the magnetic subsystem is caused also by the considerable diffusion of the phase transition of the electric subsystem (it is not observed on  $\varepsilon(T)$  graphs in PFN-MnZnFe composite of additional anomalies, occurring in PFN-NiZnFe composite).

At low temperatures and for high frequencies, the  $\tan\delta$  dielectric losses of the PFN-NiZnFe composite are low (Fig. 5a). For a frequency of 1.0 kHz up to a temperature of approx. 120°C,  $\tan\delta$  values do not exceed 0.1. However, these losses are higher than their counterparts for PFN ceramics (dashed line in Fig. 5a). Beyond the  $T_m$  phase transition, the  $\tan\delta$  values increase rapidly (increase of electric conduction). On the other hand, the dielectric losses in the PFN-MnZnFe composite are considerably higher (Fig. 5b). This is related to the properties of MnZnFe ferrite (with very low  $\rho$ ), which additionally increases the electric conduction of the entire composite, already at relatively low temperatures.

The magnetic measurements performed in the wide temperature range reveal magnetic phase transitions. Figures 6a and 6b depict the  $M(T)$  curves determined in magnetic field 0.1 T for PFN-NiZnFe and PFN-MnZnFe, respectively. The magnetic hysteresis loops (obtain at 27°C) and low temperature  $M(T)$  dependences are also included (in insets). In the case of PFN-NiZnFe, the observed T-dependent magnetization is typical for ferromagnetic materials with the Curie point (determined from the inflection point) at 390°C. The ferromagnetic state is confirmed by the  $M(T)$  curve (see inset in bottom left) i.e. saturation in relatively low fields. For the second composite (PFN-MnZnFe) the magnetic order is not obvious. One can see (in Fig. 6b) a well-defined Curie temperature (240°C) but below this point  $M(T)$  is almost linear and saturates at about -200°C. This behavior can be attributed to the ferromagnetic structure of the magnetic moments. The other possibility is a contribution of the magnetic disorder characteristic for granular magnets. Such effects should

influence the magnetization process that is shown in the  $M(T)$  curve (see inset in Fig. 6b). In fact, in the hysteresis loop the appearance of coercivity is observed.

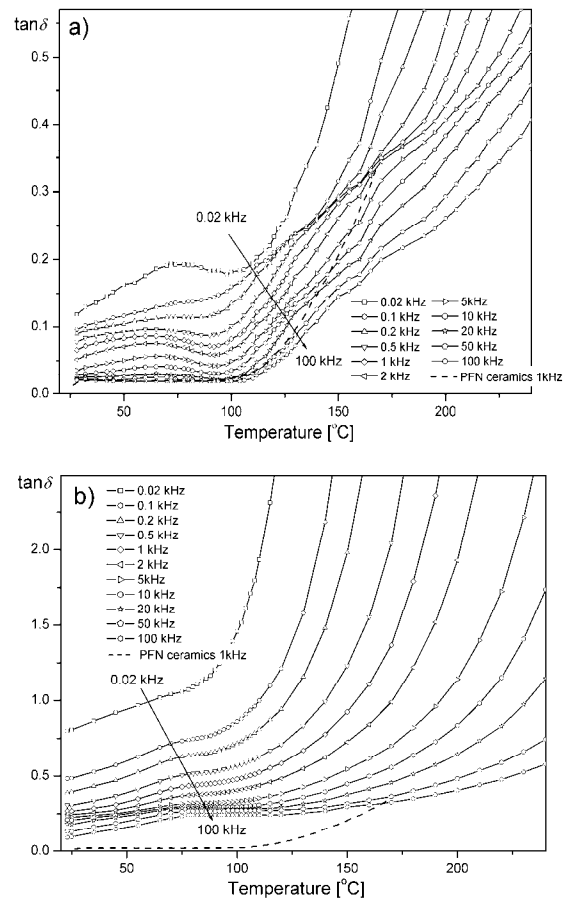


Fig. 5. Temperature dependences of  $\tan\delta$  for composite: a) PFN-NiZnFe, b) PFN-MnZnFe (heating)

Rys. 5. Temperaturowe zależności tangensa kąta strat dielektrycznych  $\tan\delta$  dla kompozytu: a) PFN-NiZnFe, b) PFN-MnZnFe (grzanie)

It is also characteristic that around the ferroelectric-paraelectric phase transitions (i.e. for PFN-NiZnFe about 98°C, for PFN-MnZnFe about 86°C - Fig. 4), one can observe some small anomalies in the thermomagnetic curves. The phase transitions settings in the studied composites, visible on the  $\varepsilon(T)$  - Figure 4 and on the  $M(T)$  - Figure 6 dependences, are also confirmed on the graphs of the dependences of the mechanical losses  $Q^{-1}$  in the temperature function (Fig. 7). The dependences were determined by the internal friction method [11].

In the field of positive temperatures, on the  $Q^{-1}(T)$  and  $Y(T)$  dependences in the area around the phase transitions, characteristic anomalies of the electric and magnetic subsystems of the ferroelectric - ferromagnetic composites are observed. In the case of the PFN-NiZnFe composite at the temperature about 98°C, the maximum  $P_p$  on the dependence  $Q^{-1}(T)$  corresponds to the minimum  $A_p$  on the dependence  $Y(T)$ , whereas in the PFN-MnZnFe composite, the maximum  $P_p$  and the minimum  $A_p$  appear at a somewhat lower temperature

(about  $86^\circ\text{C}$ ). Additionally for both composites, at higher temperatures the anomalies connected with the phase transition of their magnetic subsystem are observed: respectively at the temperature of about  $390^\circ\text{C}$  (for PFN-NiZnFe composite) and about  $230^\circ\text{C}$  (for PFN-MnZnFe composite).

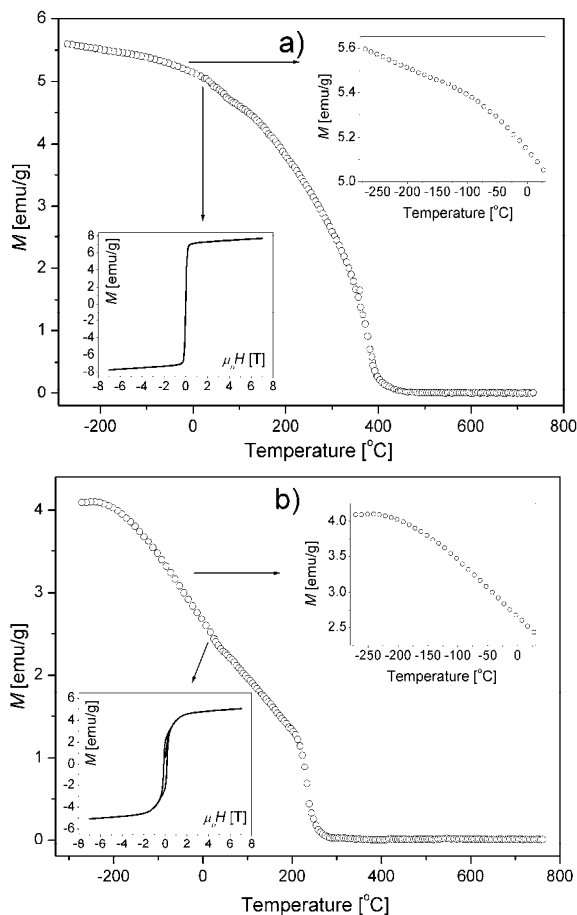


Fig. 6. Magnetization temperature dependences for composites: a) PFN-NiZnFe, b) PFN-MnZnFe (heating)

Rys. 6. Temperaturowe zależności magnetyzacji dla kompozytów: a) PFN-NiZnFe, b) PFN-MnZnFe (grzanie)

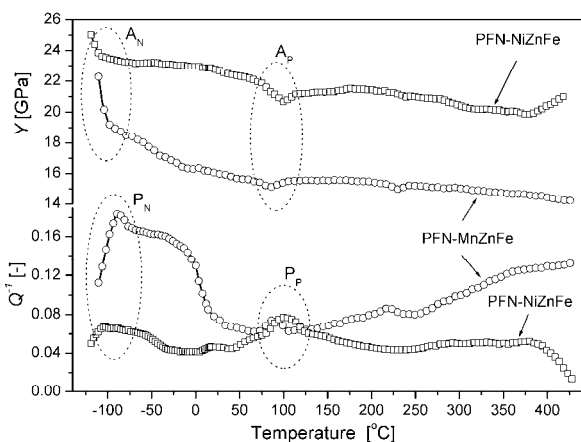


Fig. 7. Diagrams of  $Q^{-1}(T)$  and  $Y(T)$  relationships for PFN-NiZnFe and PFN-MnZnFe composites

Rys. 7. Temperaturowe zależności tarcia wewnętrznego  $Q^{-1}(T)$  oraz modułu Younga  $Y(T)$  dla kompozytów PFN-NiZnFe oraz PFN-MnZnFe

At lower (negative) temperatures, on the  $Q^{-1}(T)$  and  $Y(T)$  graphs, changes are also observed ( $P_N$  and  $A_N$  points). The changes can be connected with the additional magnetic phase transition originating from the ferroelectromagnetic component of the tested composites - PFN.

Analyzing the mechanical losses values, it is evident that the PFN-NiZnFe composite in comparison to the PFN-MnZnFe composite in the whole temperature range, has lower values of  $Q^{-1}$ . Confirmation of the temperature dependences of the dielectric losses (Fig. 5) also appears. The higher values of Young's modulus  $Y$  for the PFN-NiZnFe composite also show its better mechanical properties.

TABLE 1. Properties for PFN ceramics and composites PFN-ferrite type (dielectric parameters for  $\nu = 1$  kHz).

TABELA 1. Właściwości ceramiki PFN i kompozytów typu PFN-ferryt (parametry dielektryczne dla  $\nu = 1$  kHz)

	PFN	PFN-NiZnFe	PFN-MnZnFe
$\rho$ [g/cm <sup>3</sup> ]	8.19	7.69	7.64
$\rho_{DC}$ at $T_r$ [ $\Omega\text{m}$ ]	$5.36 \times 10^8$	$8.72 \times 10^4$	$1.98 \times 10^4$
$M_S$ [emu/g]	–	7.10	4.49
$\epsilon_r$	2,900	2,880	3,200
$T_m$ [ $^\circ\text{C}$ ]	100	98/285	86
$\epsilon_m$	9,200	17,800/9650	14,800
$\tan \delta$ at $T_r$	0.01	0.05	0.26
$\tan \delta$ at $T_m$	0.02	0.08	0.45

## SUMMARY

The carried out temperature tests of the dielectric properties of the PFN-NiZnFe composite showed the occurrence of three dielectric permittivity maxima on  $\epsilon(T)$  dependences. The first maximum, occurring at a lower temperature, is related to the ferroelectric-paraelectric phase transition; the second, related to the activation mechanism of electric conductivity and the third occurring at a higher temperature, could be related to the existence of the magnetic-paramagnetic phase transition. Studies on the magnetic properties of the composite also showed the presence (slight) of an anomaly on the  $M(T)$  graphs at those characteristic temperatures. This could show the influence of the magnetic subsystem on the electric properties of the PFN-NiZnFe composite.

In the case of the PFN-MnZnFe composite, due to the lower temperature of the magnetic transition of the MnZnFe ferrite, a simultaneous impact is observed of two subsystems (electric and magnetic) on the  $\epsilon(T)$  dependence. When comparing the two composites, it may be observed that the PFN-NiZnFe composite presents more optimum parameters. Despite the considerably lower transition temperature of the magnetic subsystem, the excessively high electric conduction of the  $\text{Mn}_{0.8}\text{Zn}_{0.2}\text{Fe}_2\text{O}_4$  ferrite (MnZnFe) eliminates it from

practical application in ferroelectric-ferromagnetic composites with optimum parameters. The polarization (using high constant polarization fields) of such composites with high electric conduction (necessary for tests on magnetoelectric properties) will not be possible.

## REFERENCES

- [1] Wang K.F., Liu J.-M., Ren Z.F., Multiferroicity: the coupling between magnetic and polarization orders, *Adv. Phys.* 2009, 58, 4, 321-448.
- [2] Schmid H., Some symmetry aspects of ferroics and single phase multiferroics, *J Phys.: Condens Matter* 2008, 20, 434201, 1-24.
- [3] Raymond O., Font R., Suarez-Almodovar N., Portelles J., Siqueiros J.M., Frequency-temperature response of ferro-electromagnetic  $\text{PbFe}_{1/2}\text{Nb}_{1/2}\text{O}_3$  ceramics obtained by different precursors. Part II. Impedance spectroscopy characterization, *J. Appl. Phys.* 2005, 97, 084108, 1-8.
- [4] Bochenek D., Relations between physical properties of the biferroic  $\text{Pb}(\text{Fe}_{1-x}\text{Nb}_x)\text{O}_3$  ceramics and their composition change, *Eur. Phys. J.-Spec. Top.* 2008, 154, 15-18.
- [5] Khomskii D., *Physics* 2009, 2, 20.
- [6] Raymond O., Font R., Suarez N., Portelles J., Siqueiros J.M., Effects of two kinds of  $\text{FeNbO}_4$  precursors in the obtainment and dielectric properties of PFN ceramics, *Ferroelectrics* 2003, 294 141-153.
- [7] Majumder S.B., Bhattacharyya S., Katiyar R.S., Manivanan A., Dutta P., Seehra M.S., Dielectric and magnetic properties of sol-gel-derived lead iron niobate ceramics, *J. Appl. Phys.* 2006, 99, 024108, 1-9.
- [8] Bochenek D., Surowiak Z., Influence of admixtures on the properties of biferroic  $\text{Pb}(\text{Fe}_{0.5}\text{Nb}_{0.5})\text{O}_3$  ceramics, *Phys Status. Solidi.* 2009, A 206, 12, 2857-2865.
- [9] Penchal Reddy M., Madhuri W., Ramamanohar Reddy N., Siva Kumar K.V., Murthy V.R.K., Ramakrishna Reddy R., Magnetic properties of Ni-Zn ferrites prepared by microwave sintering method, *J. Electroceram.* 2012, 28, 1-9.
- [10] Bochenek D., Surowiak Z., Krok-Kowalski J., Poltiero-va-Vejpravova J., Influence of the sintering conditions on the physical properties of the ceramic PFN multiferroics, *J. Electroceram.* 2010, 25, 122-129.
- [11] Bochenek D., Zachariasz R., PFN ceramics synthesized by a two-stage method, *Arch. Metall. Mater.* 2009, 54, 903-910.